LAWRENCE
LIVERMORE
NATIONAL
LABORATORY

LLNL-JRNL-648146

THEORETICAL CONFIRMATION OF GA-STABILIZED ANTI-FERROMAGNETISM IN PLUTONIUM METAL

P. Soderlind, A. Landa

January 6, 2014

Journal of Nuclear Materials

Disclaimer

Theoretical confirmation of Ga-stabilized anti-ferromagnetism in plutonium metal

Per Söderlind and Alex Landa

Condensed Matter and Materials Division, Physical and Life Sciences Directorate,

Lawrence Livermore National Laboratory, Livermore, CA 94551, USA

Corresponding authors e-mail address: soderlind@llnl.gov

Abstract

The density-functional-theory (DFT) model for plutonium metal is shown to be consistent with recent magnetic measurements that suggest anti-ferromagnetism in Pu-Ga alloys at low temperatures. The theoretical model predicts a stabilization of the face-centered-cubic (fcc, δ) form of plutonium in an anti-ferromagnetic configuration when alloyed with gallium. The ordered magnetic phase occurs because Ga removes the mechanical instability that exists for unalloyed δ-Pu. The cause of the Ga-induced stabilization is a combination of a lowering of the band (kinetic) and electrostatic (Coulomb) energies for the cubic relative to the tetragonal phase. Similarly, gallium plays an important role in stabilizing anti-ferromagnetism in the tetragonal P4/mmm Pu_3Ga compound.

I. INTRODUCTION

In addition to cerium, plutonium may well be the most complex, least understood, and most controversial elemental solid in the Periodic Table of Elements. These three attributes arise from the behavior of the 5*f* electrons and their prominence in this metal. For instance, the ground state of Pu has a low symmetry (monoclinic) and open crystal structure that is believed to exist because of narrow valence 5*f* states provide for a Jahn-Teller-like distortion of the lattice [1]. On the other hand, modest temperatures drive Pu into gradually simpler crystal structures with much larger atomic volumes that surely are due to a change in the bonding character of the 5*f* electrons. Modeling is indeed faced with great challenges when trying to capture the many facets of plutonium and its 5*f* electrons and consequently several theoretical approaches have been proposed [2]. The ground-state density-functional-theory (DFT) model has certainly overcome some of the difficulties and realistically describes chemical bonding and energetics of the all known phases of Pu, except the high-temperature body-centered cubic (bcc, ε) phase [3]. The aforementioned controversy is mostly focused on the DFT prediction of magnetism in plutonium metal [3] that has generally eluded experimental efforts [4] and motivated theoretical modeling that prohibits its existence [2].

There are, however, magnetization measurements on plutonium alloys that have been interpreted to show ordered magnetism at low temperatures [5-7]. These studies examined the face-centered cubic (δ) phase that is important from and engineering standpoint and is stable above 320 °C but can survive cooling to low temperatures when alloyed with, for example, gallium. Recent magnetization experiments [6, 7] suggest that the δ-$Pu_{92}Ga_8$ alloy undergoes a magnetic ordering transition, paramagnetic to anti-

ferromagnetic, when cooled below about 30 K. Correspondingly, the Pu_3Ga compound shows [6, 7] a slightly higher critical (Néel) temperature of the magnetic transition (40 K).

It is the fundamental purpose of the present article to explore if the first-principles DFT model is consistent with the observed magnetic behavior [5-7] of δ-Pu and particularly the Pu-Ga system including δ-$Pu_{92}Ga_8$ and Pu_3Ga. To that end, we perform electronic-structure calculations for these systems and investigate mechanical stability of the anti-ferromagnetic phase.

Section II deals with computational details for two electronic-structure methodologies we are utilizing for the problem. Section III illustrates our results and, lastly, in section IV, we discuss the results and attempt to explain them.

II. COMPUTATIONAL DETAILS

We are focusing our first-principles modeling on robust implementations of DFT from which consistent predictions can be made without the uncertainty of model parameters. Two significantly different electronic-structure codes are utilized with complimentary strengths. The full-potential linear muffin-tin orbitals (FPLMTO) method do not compromise on accuracy beyond that necessary for the electron exchange and correlation energy functional, which is chosen to be the generalized gradient approximation (GGA) [8]. Although newer varieties of this assumption have been proposed, the GGA still remains the best choice for actinide metals [9].

The other approach, the exact muffin-tin orbitals (EMTO) method, is well suited for alloy calculations because it allows for the coherent potential approximation (CPA) of

the alloy system, while alloy treatment within the FPLMTO is instead handled with a 24-atom super-cell (2 x 2 x 3). We focus on, in addition to elemental Pu, Pu_xGa_{1-x} alloys with x = 4%, 8%, and 12%. The FPLMTO alloy calculations are performed for 1, 2, and 3 Ga atoms in the 24-atom super-cell approximating 4.2%, 8.3%, and 12.5% atomic-percent Ga content while within the EMTO, CPA allows for any choice of x. In the following, when referring to 4%, 8%, and 12%, we imply these exact concentrations for EMTO but the super-cell concentrations, mentioned above, for FPLMTO.

Let us describe some of the more fundamental details of these two computational techniques.

Our particular FPLMTO implementation is based on an implementation that has recently been described in detail [10]. In addition to the choice of GGA, we know that for actinides no geometrical approximations, "full potential", full relativity including spin-orbit coupling, spin and orbital polarization, and a well converged basis set is often needed for the best accuracy. Specifically, we associate a set of 6*s* and 6*p* semi-core states in addition to the valence states (7*s*, 7*p*, 6*d*, and 5*f*) to two kinetic energy parameters for a so-called double basis set. The alloy approximation of the δ-Pu-Ga alloy system is, as mentioned, accomplished with a 24-atom super-cell and 32 k points in the irreducible part of the Brillouin zone are used for the appropriate summations. The ordered Pu_3Ga (P4/mmm) has 8 atoms per unit cell in the anti-ferromagnetic configuration and also here 32 k points are applied.

The EMTO electronic-structure method makes use of both scalar relativistic and full relativistic Green's function techniques based on the improved screened Korringa-Kohn-Rostoker (KKR), although in the present study only scalar relativistic calculations

are performed. Here, the one-electron potential is represented by optimized and overlapping muffin-tin (OOMT) potential spheres [11] where the potential is spherically symmetric and constant outside. The radius of the potential sphere, its spherical potential, and the constant value in the interstitial region are determined by minimizing the deviation between the exact and overlapping potentials, and the errors caused by the overlap between the spheres. This approximation provides for a nearly "full potential" treatment that is sufficient for the study of distorted crystal structures.

Within the EMTO formalism, the one-electron states are calculated exactly for the OOMT potentials. As an output of the EMTO calculations, one can determine the self-consistent Green's function of the system and the complete, non-spherically symmetric charge density. Finally, the total energy is calculated using the full charge-density technique [12]. The calculations are performed for a basis set including valence *spdf* orbitals. EMTO is combined with the CPA for the calculation of the total energy of chemically random alloys [13] and EMTO-CPA calculations include the Coulomb screening potential and energy [14]. For the electron exchange and correlation energy functional, the GGA is considered [8]. The screening constants are determined from super-cell calculations using the locally self-consistent Green function (LSGF) method [15].

All presented results are obtained from computations at the theoretical equilibrium lattice constants summarized in Table 1.

III. RESULTS FOR THE PU-GA ALLOY SYSTEM AND PU_3GA

It has been known for some time that density-functional theory predicts formation of spin and orbital moments in plutonium metal [3, 16]. Specifically for δ-Pu, it has been argued [3, 17] that it is paramagnetic with disordered moments and that anti-ferromagnetism is ruled out because of mechanical instability associated with a tetragonal distortion [18]. Our present hypothesis is that adding Ga to δ-Pu, in small but sufficient amounts, could remove the mechanical instability and thus allow for anti-ferromagnetic order at low temperatures as suggested experimentally [6, 7].

Modeling a solid-solution alloy is not as straightforward as the elemental metal components themselves and here we are contrasting two approaches for the alloy approximation. In the FPLMTO calculations we are applying a 24-atom super-cell of the L_{10} anti-ferromagnetic crystal, while within EMTO the CPA technique is applied. Before comparing the two alloy treatments, we must verify that the FPLMTO and EMTO are consistent for elemental Pu. In Fig. 1 we plot the scalar-relativistic energy difference, relative to the fcc energy, as functions of axial *c/a* ratio for anti-ferromagnetic Pu with FPLMTO and EMTO. Clearly, the two methods give very similar results, particularly close to the high-symmetry (*c/a* = 1.414) fcc structure. For larger tetragonal distortions (*c/a* ~ 1.3) the two methods deviate somewhat and this is likely due to FPLMTO and EMTO having different geometrical approximations for the electron charge density and potential.

Next, in Fig. 2, once again for the scalar-relativistic treatment, we compare FPLMTO and EMTO for the Pu-Ga alloy with 4, 8, and 12 atom percent Ga. In spite of the differences in electronic structure codes as well as in the explicit alloy treatments, the two approaches agree very well. This fact suggests that the DFT model is robust and

insensitive to variations between the methods and that both alloy approximations (super-cell and CPA) are appropriate in this case. It is also obvious in Fig. 2 that addition of Ga has a tendency to mitigate the tetragonal instability; the energy minimum approaches *c/a* = 1.414 (fcc) when Ga is added. But, within the scalar-relativistic model, mechanical stability never fully occurs for fcc even with higher Ga content and the results converge around 12% Ga.

The next step is to include spin-orbit interaction in the electronic structure, which we do by utilizing the FPLMTO (super-cell) method in Fig. 3. The upper (a) and lower (b) panel shows results from the scalar relativistic, and spin-orbit-interaction calculations, respectively. Notice here that including spin-orbit interaction indeed stabilizes the fcc structure at about 8% Ga (12% Ga gives very similar result). Also, for the 12% Ga alloy, adding also orbital polarization (SO+OP, dashed line), which can be very important for δ-Pu [19], does not significantly change the results and conclusion.

The DFT model is thus fully compatible with the magnetization experiments [6, 7] that suggest that δ-$Pu_{92}Ga_8$ is anti-ferromagnetic at low temperatures. The model further confirms the well-known fact that unalloyed δ-Pu is not anti-ferromagnetic and does not stabilize at lower temperatures.

Experimentally [6, 7] the ordered Pu_3Ga compound is also found to be anti-ferromagnetic at low temperatures (below 40 K). Therefore, we address the mechanical stability of Pu_3Ga in the anti-ferromagnetic configuration and plot the results in Fig. 4. These calculations include spin-orbit interaction and orbital polarization and show that the anti-ferromagnetic phase is stable with respect to a tetragonal deformation at a *c/a* axial ratio of about 1.01. The theoretical *c/a* axial ratio is in accurate accord with the

published experimental value for this compound [20] that crystallizes in a tetragonal phase (P4/mmm) with only a slight tetragonal distortion, marked with an arrow in Fig. 4.

For completion, we summarize our calculated equilibrium lattice constants and compare with available experimental data in Table 1. The overall agreement between theory and experiment is reasonable and the fact that adding Ga reduces the atomic volume in the Pu-Ga alloy system is clearly captured by the calculations. The lattice constant for Pu_3Ga is rather insensitive to computational details and also here theory compares well with handbook data.

IV. DISCUSSION

We mentioned in the introduction that distortions of the crystal structures in the actinide metals, including plutonium, are explained by narrow 5*f* states crossing the greatest occupied energy level (Fermi level) [1]. This scenario provides for a mechanism that can lower the band (kinetic) energy by reducing the crystal-structure symmetry. Hence, crystal-structure symmetry-related degenerate energy levels can be separated with some states shifted down in energy and others lifted above the Fermi level, leading to a net gain in the band energy [1]. This "Peierls distortion" mechanism is, however, counterbalanced by electrostatic atomic repulsion favoring higher symmetry atomic arrangements that helps explain why the actinides prefer cubic or hexagonal structures under compression [22].

With this in mind, it is sensible to investigate the kinetic (band) and electrostatic (Coulomb) energy contributions to the total energy in order to understand the processes that stabilizes the anti-ferromagnetic fcc phase in plutonium when alloyed with Ga. It is

understood that finding the relevant actions responsible for the fcc stabilization is challenging because the distortion energies involved are very small (Fig. 3). Indeed, comparisons of the calculated electronic density of states (DOS) reveal only obscure differences between the fcc phase and a small tetragonal distortion of it (not shown). However, we do find systematic changes of the DOS at the Fermi level, $D(E_F)$, as a function of Ga content, that illuminate the stabilization.

In Fig. 5 we display $D(E_F)$, obtained from FPLMTO calculations including spin-orbit interaction, as functions of the *c/a* axial ratio for Pu and three Pu-Ga alloys. Notice that for unalloyed Pu, a tetragonal distortion ($c/a < 1.414$) of the crystal structure results in a dramatic reduction of $D(E_F)$ whereas for the Pu-Ga alloys this behavior strongly diminishes. Because a large $D(E_F)$ is required for an efficient Peierls distortion [1], it is clear that adding Ga to Pu suppresses the tendency for deformation of the crystal. As a result, alloying imply a relative stabilization of the fcc crystal structure in the anti-ferromagnetic configuration.

In addition to the band energy contributions one suspects that also electrostatic interactions may play a role in stabilizing the anti-ferromagnetic δ-Pu-Ga alloy. Hence, we plot the electrostatic Madelung energies conveniently obtained [14] from scalar-relativistic EMTO calculations for Pu and three Pu-Ga alloys in Fig. 6. Because the electrostatic energy favors higher symmetry and closer packed crystal structures it is not surprising to find the Madelung-energy minimum close to $c/a = 1.414$ (fcc). For elemental Pu the electrostatic energy is weakly increasing for a tetragonal deformation ($c/a < 1.414$) but, interestingly, this increase is greatly amplified for the Pu-Ga alloys. Furthermore, the most dramatic change in this regard occurs already for the 4% Ga alloy

suggesting that even small amounts of Ga in Pu strongly enhance the electrostatic energies that favor the fcc phase.

The reason that electrostatic interactions are sensitive to the alloying is that the Madelung energy is proportional to the magnitude of the electronic charge transfer between the atoms [14] and it is found to be very significant from Pu to Ga in our calculations. For more details on the partition of the total energy within EMTO formalism see Refs. [11, 23].

In conclusion, the two interactions (kinetic and electrostatic) recognized to help mechanically stabilize the fcc δ phase and sustaining anti-ferromagnetism, are general in nature and not isolated only to the Pu-Ga alloy system. We are thus currently exploring other δ-Pu alloys for which anti-ferromagnetism may exist.

ACKNOWLEDGEMENTS

We thank B. Sadigh, A. Ruban and L. Vitos for helpful discussions. This work performed under the auspices of the U.S. DOE by LLNL under Contract DE-AC52-07NA27344.

References

1. P. Söderlind, O. Eriksson, B. Johansson, J. M. Wills, and A. M. Boring, Nature **374**, 524 (1995).
2. O. Eriksson, J. D. Becker, A. V. Balatsky, and J. M. Wills, J. Alloys Compd. **287**, 1 (1999); S. Y. Savrasov and G. Kotliar, Phys. Rev. Lett. **81**, 2570 (2000); A. O. Shorikov, A. V. Lukoyanov, M. A. Korotin, and V. I. Anisimov, Phys. Rev. B **72**, 024458 (2005); G. Kotliar *et al.,* Rev. Mod. Phys. **78**, 865 (2006); A. Solontsov

and V. P. Antropov, Phys. Rev. B **81**, 214402 (2010); P. Söderlind, G. Kotliar, K. Haule, P. M. Oppeneer, D. Guillaumont, MRS Bull. **35**, 883 (2010).

3. P. Söderlind, Europhysics Lett. **55**, 525 (2001); P. Söderlind and B. Sadigh, Phys. Rev. Lett. **92**, 185702 (2004).
4. J. C. Lashley, A. Lawson, R. J. McQueeney, G. H. Lander, Phys. Rev. B **72**, 054416 (2005).
5. S. Méot-Reymond, J. -M. Fournier, J. Alloys Compd. **232**, 119 (1996).
6. V. E. Arkhipov, F. A. Kassan-Ogly, A. V. Korolev, S. V. Verkhovskii, Yu. N. Zuev, and I. L. Svyatov, J. Nucl. Mater. **385**, 42 (2009).
7. F. A. Kassan-Ogly, A. V. Korolev, V. V. Ustinov, Yu. N. Zuev, and V. E. Arkhipov, Phys. Met. Metallogr. **114**, 1155 (2013).
8. J. Perdew, J. A. Chevary, S. H. Vosko, K. A. Jackson, M. R. Pederson, and D. J. Singh, Phys. Rev. B **46**, 6671 (1992).
9. P. Söderlind, O. Eriksson, B. Johansson, and J. M. Wills, Phys. Rev. B **50**, 7291 (1994); P. Söderlind and A. Gonis, Phys. Rev. B **82**, 033102 (2010).
10. J. M. Wills, M. Alouani, P. Andersson, A. Delin, O. Eriksson, and O. Grechnev, *Full-Potential Electronic Structure Method* (Springer-Verlag, Berlin, 2010).
11. L. Vitos, *Computational Quantum Mechanics for Materials Engineers: The EMTO Method and Application* (Springer-Verlag, London, 2007).
12. J. Kollar, L. Vitos, and H. L. Skriver, *Electronic Structure and Physical Properties of Solids: The Uses of the LMTO Method*, in *Lecture Notes in Physics*, edited by H. Dreyssé (Springer-Verlag, Berlin, 2000), p. 85.
13. L. Vitos, I. A. Abrikosov, and B. Johansson, Phys. Rev. Lett. **87**, 156401 (2001).

14. A. V. Ruban and H. L. Skriver, Phys. Rev. B **66**, 024201 (2002); A. V. Ruban, S. I. Simak, P. A. Korzhavyi, and H. L. Skriver, Phys. Rev. B **66**, 024202 (2002).

15. I. A. Abrikosov, S. I. Simak, B. Johansson, A.V. Ruban, and H. L. Skriver, Phys. Rev. B **56**, 9319 (1997).

16. I. V. Solovyev, A. I. Liechtenstein, V. A. Gubanov, V. P. Antropov, and O. K. Andersen, Phys. Rev B **43**, 214402 (1991).

17. P. Söderlind, A. Landa, and B. Sadigh, Phys. Rev. B **66**, 205109 (2002); A. Landa, P. Söderlind, and A. V. Ruban, J. Phys.: Condens. Matter **15**, L371 (2003).

18. G. Robert, A. Pasturel, and B. Siberchicot, J. Phys.: Condens. Matter **15**, 8377 (2003).

19. P. Söderlind, Phys. Rev. B **77**, 085101 (2008).

20. B. Hocheid, A. Tanon, and J. Despres, J. Nucl. Mater. **15**, 241 (1965).

21. O. J. Wick, *Plutonium Handbook A Guide to the Technology* (Gordon and Breach, New York, 1967).

22. P. Söderlind, Adv. Phys. **47**, 959 (1998).

23. A. Landa, P. Söderlind, O. I. Velikokhatnyi, I. I. Naumov, A. V. Ruban, O. E. Peil, and L. Vitos, Phys. Rev. B **82**, 144114 (2010).

Table Captions

Table 1. Present theoretical and measured [6, 20, 21] equilibrium atomic volumes, in units of $Å^3$, for the fcc δ-Pu-Ga system. Percentages refer to the Ga-atom content in the δ-Pu-Ga alloy. The FPLMTO results denoted "SO" include spin-orbit interaction and "SO+OP" also orbital polarization.

Table 1.

Method	0%	4%	8%	12%	Pu_3Ga
FPLMTO	23.3	23.1	22.7	22.3	23.3
FPLMTO+SO	23.7	23.3	23.0	22.7	23.3
FPLMTO+SO+OP	24.7	–	–	24.0	23.6
EMTO	24.7	24.0	23.5	23.2	–
Experiment	24.9	–	23.9	–	23.1

Figure Captions

Figure 1. (Color online). Calculated scalar-relativistic FPLMTO (red, solid squares) and EMTO (black, solid circles) total energies, relative to that of fcc, as functions of *c/a* axial ratio for Pu. The vertical dashed line indicates the fcc crystal structure and lines connecting the symbols are guides to the eye only.

Figure 2. (Color online). Calculated scalar-relativistic FPLMTO (red, solid squares) and EMTO (black, solid circles) total energies, relative to that of fcc, as functions of *c/a* axial ratio for (a) δ-$Pu_{96}Ga_4$, (b) δ-$Pu_{92}Ga_8$, and (c) δ-$Pu_{88}Ga_{12}$. The vertical dashed line indicates the fcc crystal structure and lines connecting the symbols are guides to the eye only.

Figure 3. (Color online). Calculated (FPLMTO) total energies, relative to that of fcc, as functions of axial *c/a* ratio for unalloyed Pu and three Pu-Ga alloys. The upper panel (a) shows results from a scalar relativistic treatment while for the lower panel (b) spin-orbit interaction is included in the calculations. For comparison, one set of calculations (12% Ga) is performed including orbital polarization (dotted line, no symbols) in panel (b). The vertical dashed line indicates the fcc crystal structure and lines connecting the symbols are guides to the eye only.

Figure 4. (Color online). Calculated (FPLMTO) total energies, relative to that of fcc, as functions of axial *c/a* ratio for Pu_3Ga. The calculations include spin-orbit interaction (SO, open black squares) and orbital polarization (SO+OP, red solid circles). The experimental

[20] *c/a* axial ratio is highlighted with an arrow. The vertical dashed line indicates the cubic Cu_3Au phase and lines connecting the symbols are guides to the eye only.

Figure 5. (Color online). Calculated (FPLMTO) density of states at the Fermi level, $D(E_F)$, relative to that of fcc, as functions of *c/a* axial ratio for unalloyed Pu and three Pu-Ga alloys. The calculations include spin-orbit interaction. The vertical dashed line indicates the fcc crystal structure and lines connecting the symbols are guides to the eye only.

Figure 6. (Color online). Calculated (EMTO) electrostatic (Madelung) energies, relative to that of fcc, as functions of *c/a* axial ratio for unalloyed Pu and three Pu-Ga alloys. The calculations are scalar relativistic. The vertical dashed line indicates the fcc crystal structure and lines connecting the symbols are guides to the eye only.

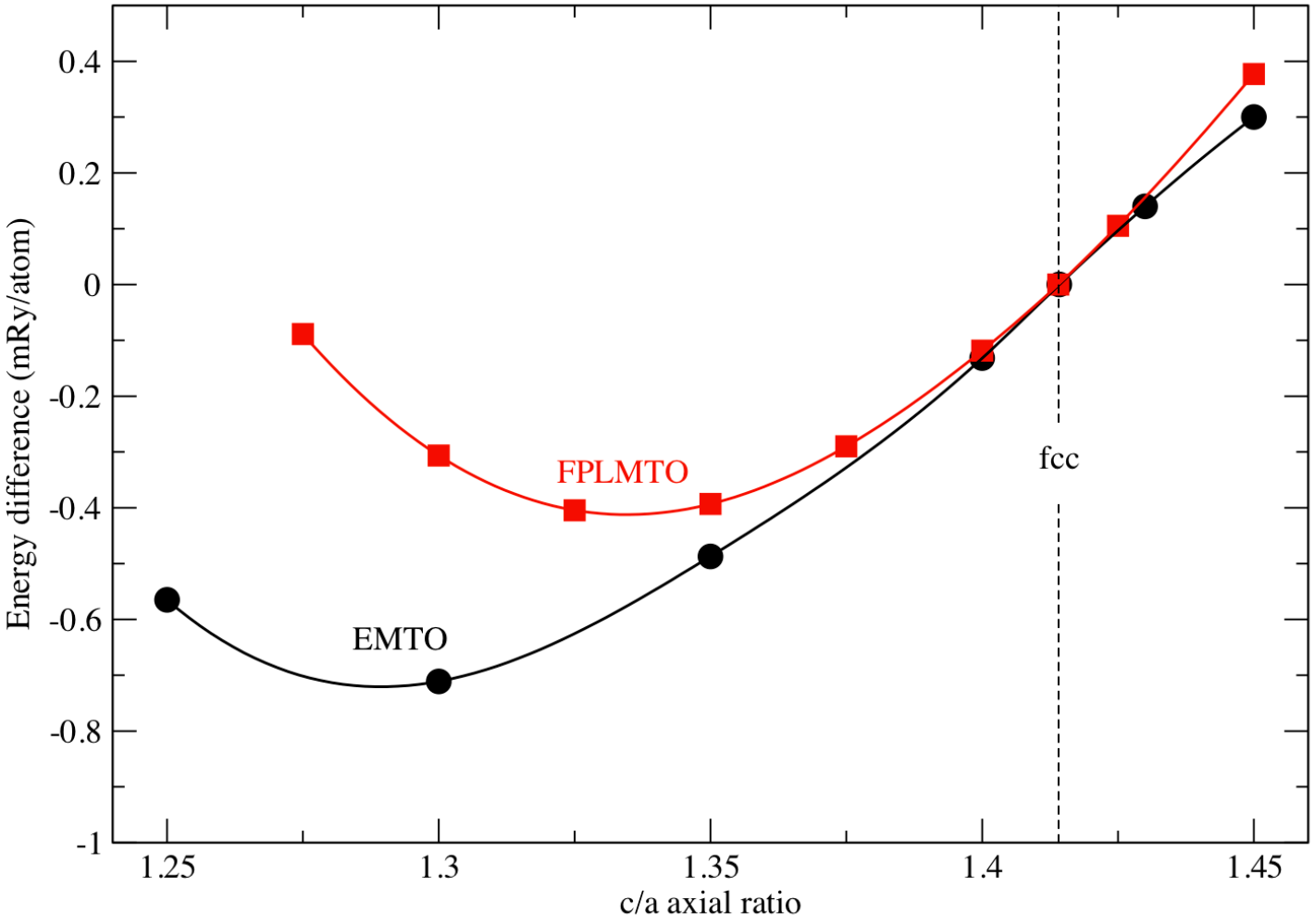
0.4
0.2
0
-0.2
-0.4
-0.6
-0.8
-1
Energy difference (mRy/atom)
1.25
1.3
1.35
1.4
1.45
c/a axial ratio
FPLMTO
EMTO
fcc

Figure 1.

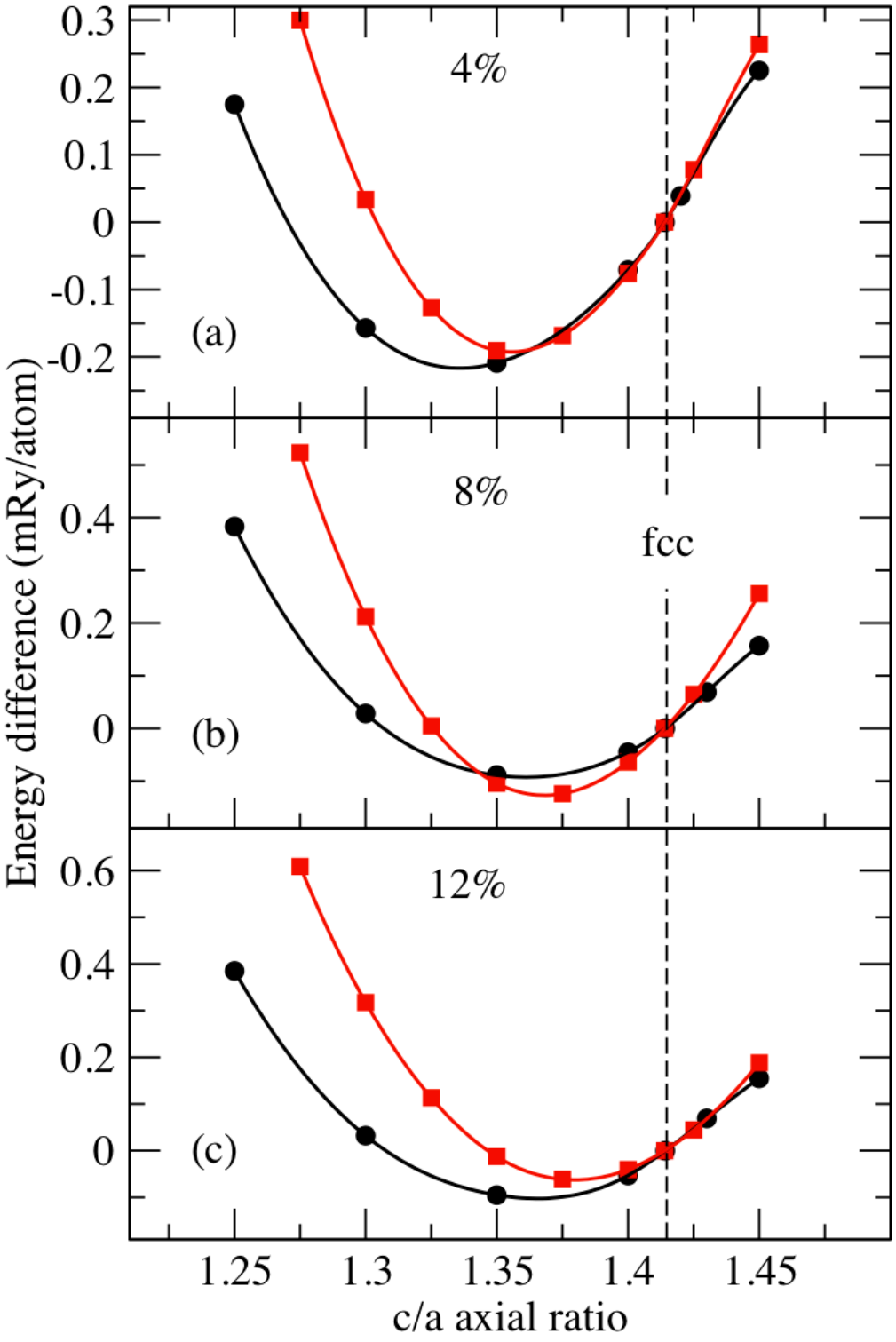
0.3
0.2
0.1
0
-0.1
-0.2
4%
(a)
0.4
0.2
0
8%
fcc
(b)
0.6
0.4
0.2
0
12%
(c)
Energy difference (mRy/atom)
1.25
1.3
1.35
1.4
1.45
c/a axial ratio

Figure 2.

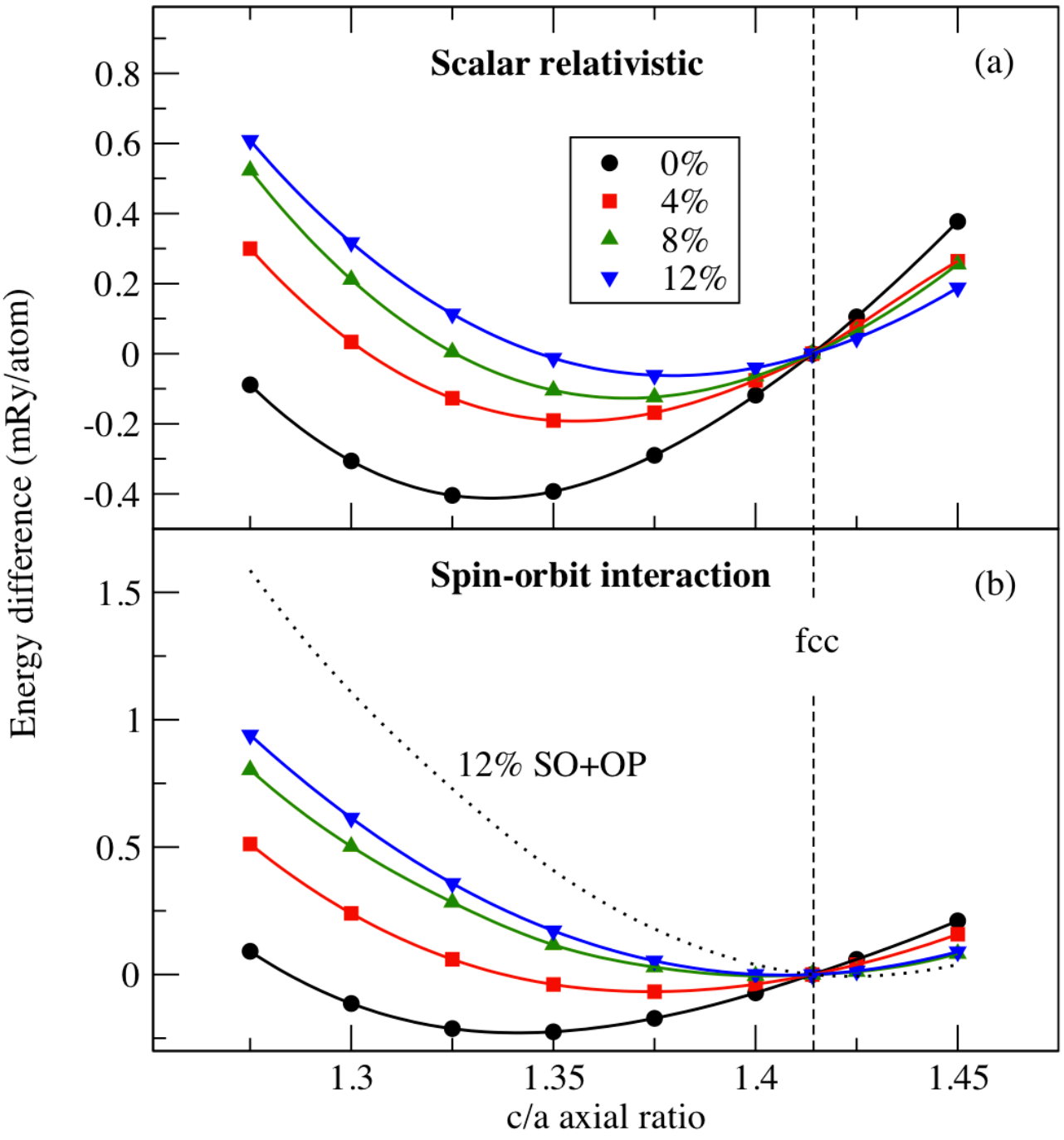
Scalar relativistic
(a)
0%
4%
8%
12%
Spin-orbit interaction
(b)
fcc
12% SO+OP
Energy difference (mRy/atom)
c/a axial ratio
0.8
0.6
0.4
0.2
0
-0.2
-0.4
1.5
1
0.5
0
1.3
1.35
1.4
1.45

Figure 3.

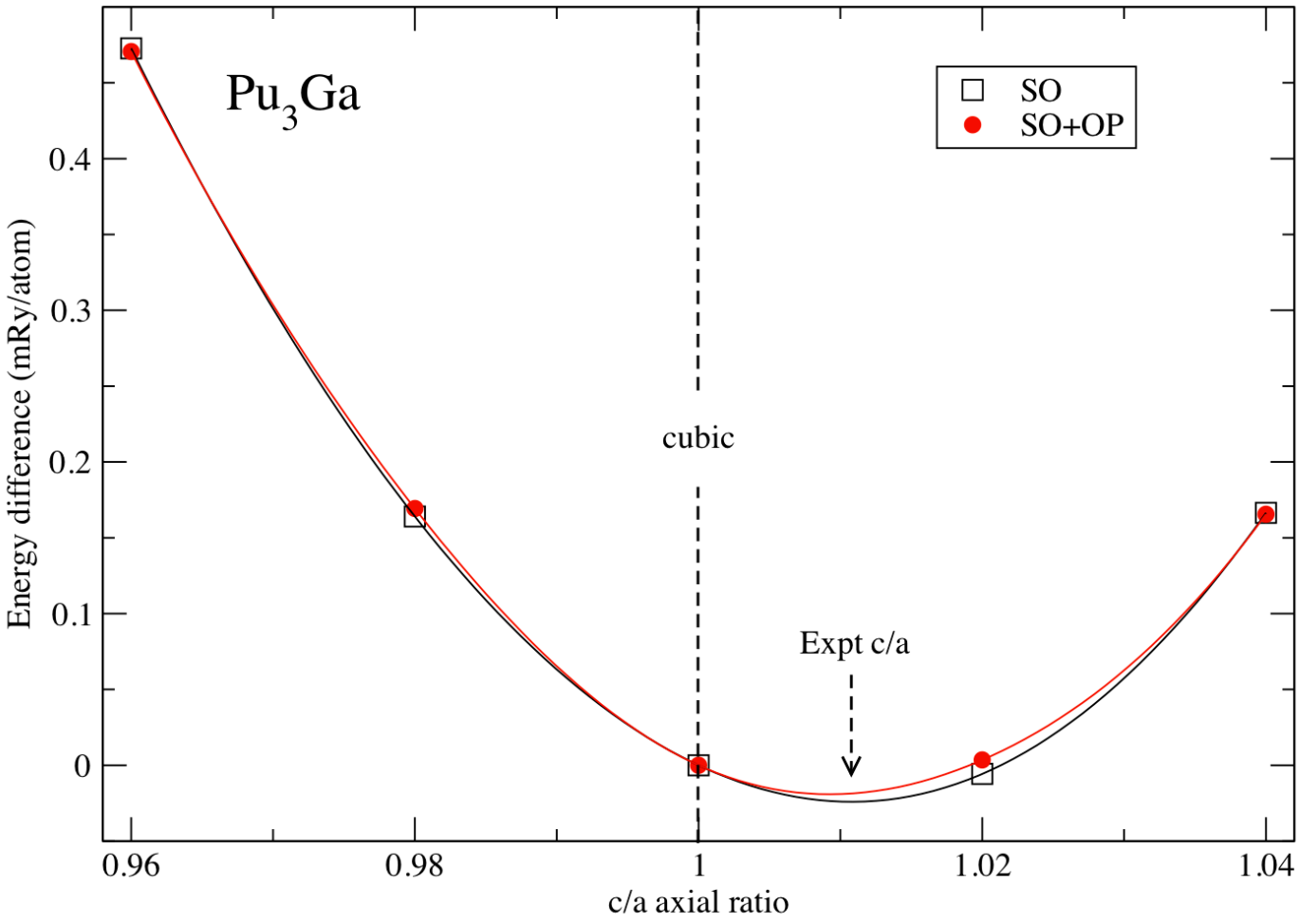
Pu3Ga
SO
SO+OP
cubic
Expt c/a
Energy difference (mRy/atom)
0.4
0.3
0.2
0.1
0
0.96
0.98
1
1.02
1.04
c/a axial ratio

Figure 4.

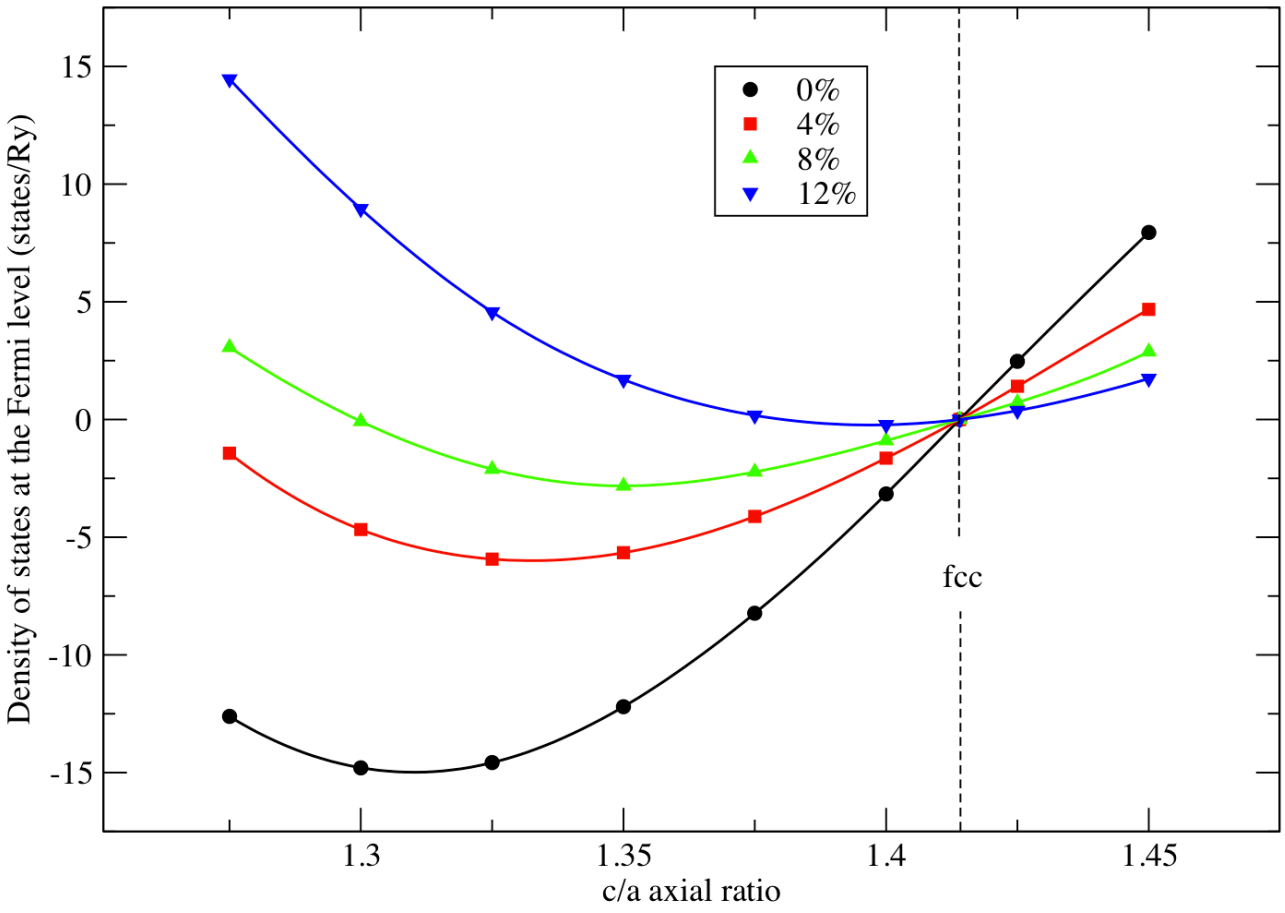
15
10
5
0
-5
-10
-15
1.3
1.35
1.4
1.45
c/a axial ratio
Density of states at the Fermi level (states/Ry)
0%
4%
8%
12%
fcc

Figure 5.

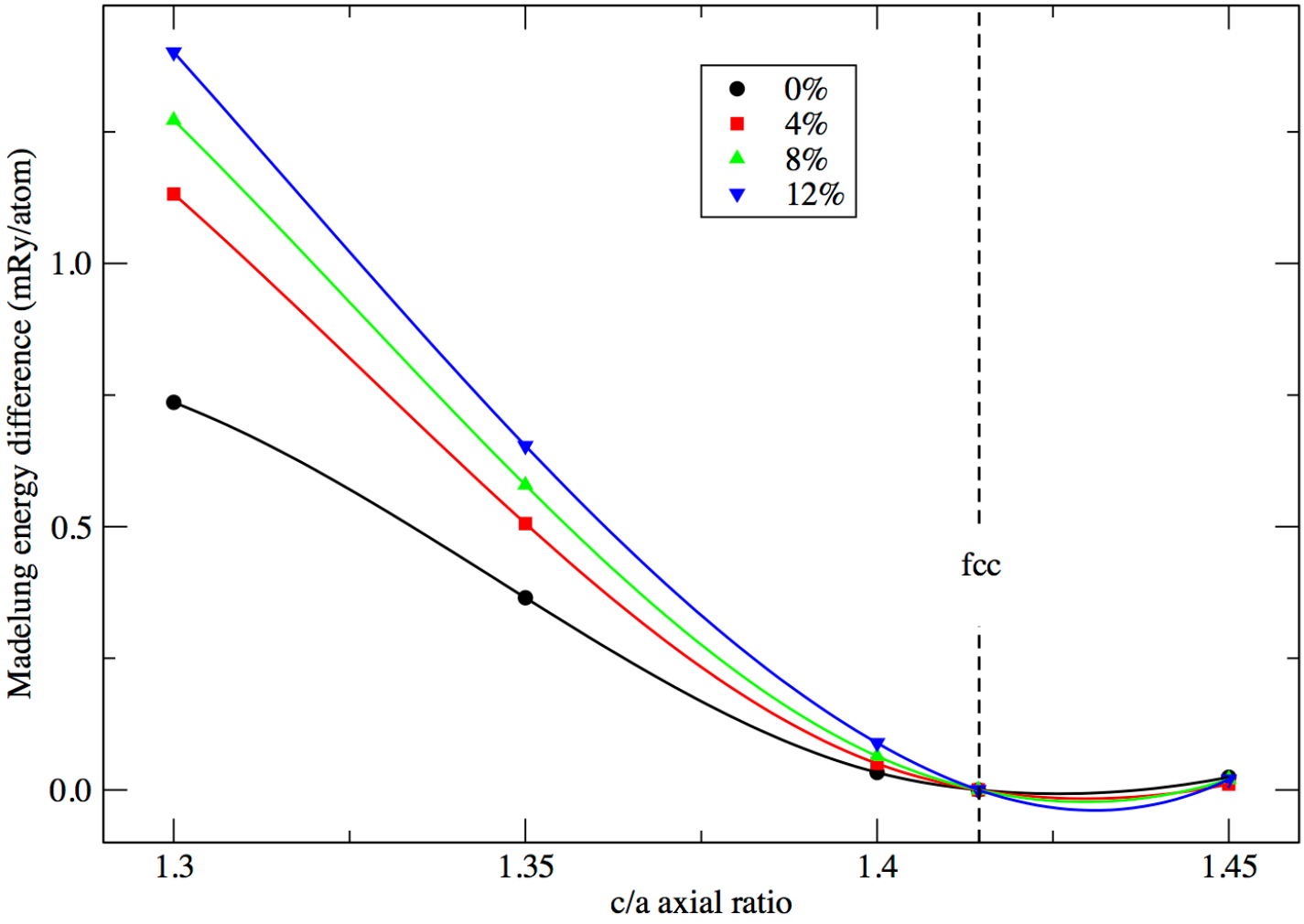
0%
4%
8%
12%
fcc
Madelung energy difference (mRy/atom)
1.0
0.5
0.0
1.3
1.35
1.4
1.45
c/a axial ratio

Figure 6.